

Constraining a possible time variation of the gravitational constant G with terrestrial nuclear laboratory data

Plamen G. Krastev and Bao-An Li

*Department of Physics, Texas A&M University – Commerce, Commerce, TX 75429, U.S.A**

(Dated: August 5, 2021)

Abstract

Testing the constancy of the gravitational constant G is a longstanding fundamental question in natural science. As first suggested by Jofré, Reisenegger and Fernández [1], Dirac’s hypothesis of a decreasing gravitational constant G with time due to the expansion of the Universe would induce changes in the composition of neutron stars, causing dissipation and internal heating. Eventually, neutron stars reach their quasi-stationary states where cooling, due to neutrino and photon emissions, balances the internal heating. The correlation of surface temperatures and radii of some old neutron stars may thus carry useful information about the rate of change of G . Using the density dependence of the nuclear symmetry energy, constrained by recent terrestrial laboratory data on isospin diffusion in heavy-ion reactions at intermediate energies, and the size of neutron skin in ^{208}Pb , within the *gravitochemical heating* formalism developed by Jofré et al. [1], we obtain an upper limit for the relative time variation $|\dot{G}/G|$ in the range $(4.5 - 21) \times 10^{-12} \text{yr}^{-1}$.

PACS numbers: 25.70.-z, 91.10.Op, 06.20.Jr, 97.60.Jd

*P. G. Krastev: Plamen.Krastev@tamu-commerce.edu; Bao-An Li: Bao-An.Li@tamu-commerce.edu

I. INTRODUCTION

The question whether or not the fundamental constants of nature vary with time has been of considerable interest in physics. The constancy of the gravitational coupling parameter G was first addressed in 1937 by Dirac [2] who suggested that the gravitational force might be weakening due to the expansion of the universe. Although general relativity assumes a strictly constant G , time variations of the Newton's constant are predicted by some alternative theories of gravity [3] and a number of modern cosmological models [5, 6]. Many theoretical approaches, such as models with extra dimensions [7], string theories [8, 9, 10], and scalar-tensor quintessence models [11, 12, 13, 14, 15, 16], have been proposed in which the gravitational coupling parameter becomes a time-dependent quantity. Nowadays the debate over the constancy of G has been revived by recent astronomical observations [19, 20] of distant high-red-shift type Ia supernovae suggesting that presently the Universe is in a state of accelerated expansion [6]. This acceleration can be interpreted in terms of a “dark energy” with negative pressure, or alternatively by allowing a time variation of the gravitational constant [4]. Soon after Dirac had published his hypothesis [2], Chandrasekhar [17] and Kothari [18] pointed out that a decreasing G with time could have some detectable astrophysical consequences. Since then many attempts have been made to find astrophysical signs due to the possible time variation of G . However, there is no firm conclusion so far (see Ref. [21] for a review). Interestingly though, as pointed out by Uzan [21], contrary to most of the other fundamental constants, as the precision of the measurements increased the discrepancy among the measured values of G also increased. This circumstance led *CODATA* (Committee on Data for Science and Technology) to raise the relative uncertainty for G [21] by a factor of about 12 in 1998. Some of the previous upper limits on the time variation of G , as obtained by different experiments/methods, are summarized in Table 1 (adapted from Reisenegger et al. [69]). Given the current status of both theory and experiment, it is fair to say that whether or not the gravitational constant varies with time is still an open question and therefore additional work is necessary to investigate further this fundamental issue.

Recently a new method, called *gravitochemical heating* [1], has been introduced to constrain a hypothetical time variation in G , most frequently expressed as $|\dot{G}/G|$. In Ref. [1] the

TABLE 1: Upper bounds on the time variations of G (adapted from Reisenegger et al. [69]). The first column lists the method used. The second column contains the upper limit on the time variation of G , most usefully expressed as $|\dot{G}/G|$, the third column is a rough time scale over which each experiment is averaging this variation, and the last column is the corresponding reference. The first two experiments on the list probe the variation of G from the early Universe to the present time. The next four experiments are sensitive to long time-scales, but without reaching to the early Universe. And the last three experiments on the list probe the change of G over short time-scales of years and decades.

Method	$ \dot{G}/G _{max}[10^{-12}yr^{-1}]$	Time scale [yr]	Reference
Big Bang Nucleosynthesis	0.4	1.4×10^{10}	[70]
Microwave Background	0.7	1.4×10^{10}	[71]
Gloubular Cluster Isochrones	35	10^{10}	[72]
Binary Neutron Star Masses	2.6	10^{10}	[73]
Helioseismology	1.6	4×10^9	[74]
Paleontology	20	4×10^9	[75]
Lunar Laser Ranging	1.3	24	[76]
Binary Pulsar Orbits	9	8	[77]
White Dwarf Oscillations	250	25	[78]

authors suggested that such a variation of the gravitational constant would perturb the internal composition of a neutron star, producing entropy which is partially released through neutrino emission, while a similar fraction is eventually radiated as thermal photons. A constraint on the time variation of G is achieved via a comparison of the predicted surface temperature with the available empirical value of an old neutron star [22]. The gravitochemical heating formalism is based on the results of Fernández and Reisenegger [24] (see also [25]) who demonstrated that internal heating could result from spin-down compression in a rotating neutron star (*rotochemical heating*). In both cases (gravito- and rotochemical heatings) predictions rely heavily on the equation of state (EOS) of stellar matter used to calculate the neutron star structure. Accordingly, detailed knowledge of the EOS is critical

for setting a reliable constraint on the time variation of G . The global properties of neutron stars such as masses, radii, moments of inertia, thermal evolution, etc have been studied extensively, see, e.g., [26, 27, 28, 29, 30, 31, 32, 34]. Generally, predictions differ widely, mainly, due to the uncertainties of the equations of state employed in neutron star structure calculations [34]. Therefore, determining the EOS of stellar matter is a question of central importance with an answer requiring understanding of proper nuclear physics.

Using the well tested parabolic approximation the EOS of isospin asymmetric nuclear matter is written as

$$e(\rho, \alpha) = e(\rho, 0) + e_{sym}(\rho)\alpha^2, \quad (1)$$

which manifests the separation of the EOS into isospin symmetric (the energy per particle of symmetric nuclear matter) and isospin asymmetric contributions (the nuclear symmetry energy e_{sym}). In the above expression $\alpha = (\rho_n - \rho_p)/\rho$ is the usual asymmetry parameter, $\rho = \rho_n + \rho_p$ is the baryon number density, and ρ_n and ρ_p are the neutron and proton densities respectively. While the EOS of symmetric nuclear matter ($\alpha = 0$) is relatively well understood, the density dependence of the symmetry energy, e_{sym} , is still very poorly constrained especially at high densities. Variations in the e_{sym} predicted by various models often yield dramatically different predictions for properties of neutron stars (e.g., see Ref. [34]). Because of its importance for neutron star structure, determining the density dependence of the symmetry energy has been a high-priority goal for the intermediate energy heavy-ion community. Although extracting the symmetry energy is not an easy task due to the complicated role of isospin in reaction dynamics, several promising probes of the symmetry energy have been suggested [35, 36, 37, 38] (see also Refs. [39, 40, 41] for reviews).

Some significant progress has been made recently in determining the density dependence of e_{sym} using: (1) isospin diffusion in heavy-ion reactions at intermediate energies as a probe of both the magnitude and slope of the symmetry energy around the saturation density ($\rho_0 \approx 0.16 \text{ fm}^{-3}$) [42, 43, 44, 45, 46, 47], (2) flow in heavy-ion collisions at higher energies to constrain the equation of state of symmetric nuclear matter [40], and (3) the sizes of neutron skins in heavy nuclei to constrain $e_{sym}(\rho)$ at subsaturation densities [32, 48, 49, 50].

In this work, we combine recently obtained diffusion data, information from flow observables, studies on the neutron skin of ^{208}Pb , and other information to constrain a possible time-variation of the gravitational constant G through the gravitochemical formalism [1].

We do not aim to add anything fundamental to the original method of Ref. [1]. Our objective is to provide a restrictive upper limit for the time variation of G , applying an EOS constrained by terrestrial empirical data from nuclear reactions induced by neutron-rich nuclei. After the introductory notes in this section, we discuss, in some details, the general formalism of the gravitochemical method. The equations of state used in this study are outlined briefly in Section III. Our results for the upper limits of $|\dot{G}/G|$ are presented and discussed in Section IV. The effects of “exotic” (hyperonic/quark) phases in neutron star matter on a possible time variation of G are addressed in Section V. We conclude in Section VI with a short summary.

II. GRAVITOCHEMICAL HEATING: FORMALISM

To provide the reader with a self-contained manuscript, in this section we recall the main steps leading to the calculation of the surface temperature of an old neutron star via the gravitochemical heating method. For a detailed discussion see Refs. [1, 24]. (Conventions and notation as in the above references.) The simplest neutron star models assume a composition of nucleons and light leptons, electrons and muons, which can transform into each other through direct and inverse β -reactions. The neutrinos (ν) and antineutrinos ($\bar{\nu}$) produced in these reactions leave the star without further interactions, contributing to its cooling. In β -equilibrium the balance between the rates of direct and inverse processes is reflected through the following relation among the chemical potentials of the particle species

$$\mu_n - \mu_p = \mu_e = \mu_\mu \quad (2)$$

As pointed out in Ref. [1] a time-variation of G would cause continuously a perturbation in the stellar density and since the chemical potentials are density-dependent the star thus always departs from β -equilibrium. This departure is quantified by the chemical imbalances

$$\eta_{npe} = \delta\mu_n - \delta\mu_p - \delta\mu_e \quad (3)$$

$$\eta_{np\mu} = \delta\mu_n - \delta\mu_p - \delta\mu_\mu \quad (4)$$

where $\delta\mu_i = \mu_i - \mu_i^{eq}$ is the deviation of the chemical potential of particle species i ($i = n, p, e, \mu$) from its equilibrium value at a given pressure. The chemical imbalances enhance

the rates of reactions driving the star to a new equilibrium state. If G changes continuously with time the star will be always out of equilibrium, storing an excess of energy that is dissipated as internal heating and enhanced neutrino emission [1].

The evolution of the internal temperature is given by the thermal balance equation

$$\dot{T}^\infty = \frac{1}{C}[L_H^\infty - L_\nu^\infty - L_\gamma^\infty] \quad (5)$$

where C is the total heat capacity of the star, L_H^∞ is the total power released by heating mechanisms, L_ν^∞ is the total neutrino luminosity, and L_γ^∞ is the photon luminosity (“ ∞ ” labels the quantities as measured by a distant observer). The evolution of the red-shifted chemical imbalances is governed by

$$\dot{\eta}_{npe}^\infty = \delta\dot{\mu}_n^\infty - \delta\dot{\mu}_p^\infty - \delta\dot{\mu}_e^\infty \quad (6)$$

$$\dot{\eta}_{np\mu}^\infty = \delta\dot{\mu}_n^\infty - \delta\dot{\mu}_p^\infty - \delta\dot{\mu}_\mu^\infty \quad (7)$$

These equations can be written as [1]

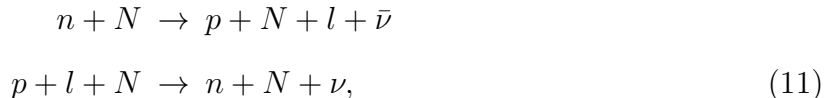
$$\dot{\eta}_{npe}^\infty = - [A_{D,e}(\eta_{npe}^\infty, T^\infty) + A_{M,e}(\eta_{npe}^\infty, T^\infty)] - [B_{D,e}(\eta_{np\mu}^\infty, T^\infty) + B_{M,e}(\eta_{np\mu}^\infty, T^\infty)] \quad (8)$$

$$\dot{\eta}_{np\mu}^\infty = - [A_{D,\mu}(\eta_{npe}^\infty, T^\infty) + A_{M,\mu}(\eta_{npe}^\infty, T^\infty)] - [B_{D,\mu}(\eta_{np\mu}^\infty, T^\infty) + B_{M,\mu}(\eta_{np\mu}^\infty, T^\infty)] \quad (9)$$

The functions A and B quantify the effect of reactions toward restoring chemical equilibrium, and thus have the same sign as η_{npl} ($l = e, \mu$) [24]. The subscripts D refers to the so-called direct Urca cooling processes



which are fast but possibly forbidden by the energy-momentum conservations when the proton fraction is low [29]. The subscripts M refers to the modified Urca reactions



which are slow and an additional nucleon or nucleus N must participate in order to conserve momentum [29]. The constants C_{npe} and $C_{np\mu}$ quantify the departure from chemical

equilibrium due to a time-variation of G . They can be written as [1]

$$\begin{aligned} C_{npe} &= (Z_{npe} - Z_{np})I_{G,e} + Z_{np}I_{G,p} \\ C_{np\mu} &= (Z_{np\mu} - Z_{np})I_{G,\mu} + Z_{np}I_{G,p} \end{aligned} \quad (12)$$

Here $I_{G,i} = (\partial N_i^{eq} / \partial G)_A$ is the change of the equilibrium number of particle species i ($i = n, p, e, \mu$), N_i^{eq} , due to the variation of G and Z are constants depending only on the stellar structure [1]. Equations (5), (8), and (9) determine completely the thermal evolution of a neutron star with gravitochemical heating. The main consequence of this mechanism is that eventually the star arrives at a quasi-equilibrium state, with heating and cooling balancing each other [1]. The properties of this stationary state can be obtained by solving simultaneously Eqs. (5), (8), and (9) by setting $\dot{T}^\infty = \dot{\eta}_{npe}^\infty = \dot{\eta}_{np\mu}^\infty = 0$. The existence of a quasi-equilibrium state makes it possible, for a given value of $|\dot{G}/G|$, to compute the temperature of an old neutron star without knowing its exact age [1], since, due to the independence of the solution from the initial conditions, it is unnecessary to model the complete evolution of the chemical imbalances and temperature.

If only the modified Urca reactions are allowed, for a given stellar model, it is possible to derive an analytic expression relating the photon luminosity in the stationary state, $L_{\gamma,eq}^\infty$, to $|\dot{G}/G|$. This is because the longer time scale required to reach a stationary state, when only modified Urca processes operate, results in chemical imbalances satisfying $\eta_{npl} \gg k_B T$ [1]. Under these conditions the photon luminosity in the quasi-equilibrium state is given by

$$L_{\gamma,eq}^\infty = C_M \left(\frac{k_B G}{C_H} \right)^{8/7} \left[\left(\frac{I_{G,e}^8}{\tilde{L}_{Me}} \right)^{1/7} + \left(\frac{I_{G,\mu}^8}{\tilde{L}_{M\mu}} \right)^{1/7} \right] \left| \frac{\dot{G}}{G} \right|^{8/7} \quad (13)$$

The meaning of the constants C_M and C_H , and the functions \tilde{L}_{M_i} ($i = e, \mu$) is explained in Refs. [1, 24]. From $L_{\gamma,eq}^\infty$ the neutron-star surface temperature can be calculated by assuming an isotropic blackbody spectrum

$$L_{\gamma,eq}^\infty = 4\pi\sigma R_\infty^2 (T_s^\infty)^4 \quad (14)$$

with σ the Stefan-Boltzmann constant and R_∞ the red-shifted radius of the star. In the case when only slow β -reactions operate, we write the stationary surface temperature as

$$T_s^\infty = \tilde{D} \left| \frac{\dot{G}}{G} \right|^{2/7}, \quad (15)$$

where the function $\tilde{\mathcal{D}}$ is a quantity depending only on the stellar model and the equation of state. On the other hand, if at higher densities the proton fraction is large enough so that the direct Urca reactions are allowed, the thermal evolution of a neutron star with gravitochemical heating needs to be modeled by solving numerically the coupled Eqs. (5), (8) and (9).

As demonstrated by Jofré et al. [1] the formalism outlined here can be applied to constrain the value of $|\dot{G}/G|$, provided one knows (i) the surface temperature of a neutron star, and (ii) that the star is certainly older than the time-scale necessary to reach a quasi-stationary state. So far the only object satisfying both conditions is PSR J0437-4715, which is the closest millisecond pulsar to our solar system. Its surface temperature was deduced from ultraviolet observations [22] while its mass was determined by Hotan et al. [79] to be in the range $M_{PSR} = (1.1 - 1.5)M_{\odot}$. (Another mass constraint, $M_{PSR} = 1.58 \pm 0.18M_{\odot}$, was given previously by van Straten et al. [23].) To constrain the value of $|\dot{G}/G|$ one, therefore, needs to consider neutron-star models in the above mass range and calculate the surface temperature for each stellar configuration.

III. EQUATION OF STATE AND NEUTRON STAR STRUCTURE

Clearly, predictions of the surface temperature and, in turn, value of $|\dot{G}/G|$ depend heavily on the EOS of neutron-star matter since the later is critical for determining the neutron-star structure. Currently, theoretical predictions of the EOS of neutron-rich matter diverge widely mainly due to the uncertain density dependence of the nuclear symmetry energy. Consequently, to provide a stringent constraint on the time variation of G , one should attempt to reduce the uncertainty due to the $e_{sym}(\rho)$. Recently available nuclear reaction data allowed us to constrain significantly the density dependence of the symmetry energy mostly in the sub-saturation density region. While high energy radioactive beam facilities under construction will provide a great opportunity to pin down the high density behavior of the nuclear symmetry energy in the future. In this work, we apply the gravitochemical method with several EOSs describing matter of purely nucleonic ($npe\mu$) as wells as hyperonic and hybrid stars. Among the nucleonic matter EOSs, we pay special attention to the one calculated with the MDI interaction [53]. The symmetry energy $e_{sym}(\rho)$ of the MDI EOS

is constrained in the sub-saturation density region by the available nuclear laboratory data, while in the high-density region we assume a continuous density functional. The EOS of symmetric matter $e(\rho, 0)$ for the MDI interaction is constrained up to about five times the normal nuclear matter density by the available data on collective flow in relativistic heavy-ion reactions.

Let us first briefly recall here the main ingredients of the MDI EOS following Ref. [52]. The MDI EOS corresponds to the single-particle potential

$$\begin{aligned}
U(\rho, \alpha, \vec{p}, \tau, x) = & A_u(x) \frac{\rho_{\tau'}}{\rho_0} + A_l(x) \frac{\rho_{\tau}}{\rho_0} + B \left(\frac{\rho}{\rho_0} \right)^{\sigma} (1 - x\alpha^2) - 8\tau x \frac{B}{\sigma + 1} \frac{\rho^{\sigma-1}}{\rho_0^{\sigma}} \alpha \rho_{\tau'} \\
& + \frac{2C_{\tau, \tau}}{\rho} \int d^3 p' \frac{f_{\tau}(\vec{r}, \vec{p}')}{1 + (\vec{p} - \vec{p}')^2 / \Lambda} + \frac{2C_{\tau, \tau'}}{\rho} \int d^3 p' \frac{f_{\tau'}(\vec{r}, \vec{p}')}{1 + (\vec{p} - \vec{p}')^2 / \Lambda}, \quad (16)
\end{aligned}$$

deduced [53] from the Gogny interaction. In the above equation x is a parameter introduced to reflect the largely uncertain density dependence of the $e_{sym}(\rho)$ as predicted by various many-body approaches; $\tau(\tau')$ is $1/2$ ($-1/2$) for neutrons (protons) with $\tau \neq \tau'$; $\sigma = 4/3$, $f_{\tau}(\vec{r}, \vec{p})$ is the space distribution function at coordinate \vec{r} and momentum \vec{p} ; A_u , A_l , B , $C_{\tau, \tau}$, $C_{\tau', \tau'}$ and Λ are parameters fixed by fitting the momentum dependence of $U(\rho, \alpha, \vec{p}, \tau, x)$, as predicted by the Gogny/Hartree-Fock and/or Brueckner-Hartree-Fock (BHF) calculations, so that the saturation properties of nuclear matter and the value of the symmetry energy at the saturation density ($e_{sym}(\rho_0) \approx 32 \text{ MeV}$) are predicted correctly. The compression modulus of saturated nuclear matter, κ , is set to 211 MeV consistent with the empirical range recently suggested by Garg [54]. More specifically, $B = 106.35 \text{ MeV}$ and $\Lambda = k_F^0$ is the nucleon Fermi momentum in symmetric nuclear matter. The quantities $A_u(x)$ and $A_l(x)$ depend on the parameter x according to

$$A_u(x) = -95.98 - x \frac{2B}{\sigma + 1} \quad (17)$$

$$A_l(x) = -120.57 + x \frac{2B}{\sigma + 1} \quad (18)$$

The isoscalar potential, evaluated from $U_0 = (U_n + U_p)/2$, agrees very well with predictions from many-body variational [55] and recent Dirac-Brueckner-Hartree-Fock (DBHF) [56] calculations. The underlying EOS has been also successfully tested against nuclear collective flow data in relativistic heavy-ion reactions at densities up to $5\rho_0$ ($\rho_0 \approx 0.16 \text{ fm}^{-3}$) [40, 57, 58, 59]. Also the strength of the symmetry potential estimated from the

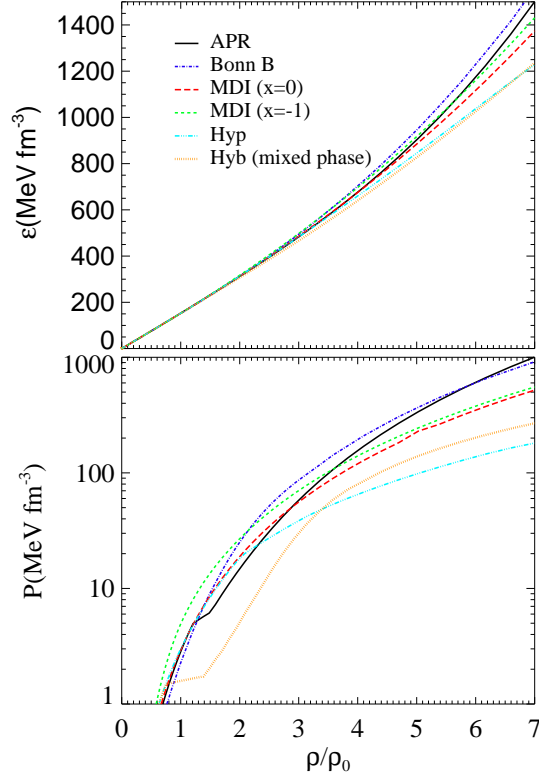


FIG. 1: (Color online) Equation of state of stellar matter in β -equilibrium. The upper panel shows the total energy density and lower panel the pressure as function of the baryon number density (in units of ρ_0).

single-nucleon potentials via $U_{sym} = (U_n - U_p)/(2\alpha)$ at ρ_0 agrees very well with the Lane potential extracted from nucleon-nucleus scatterings and (p, n) charge exchange reactions up to 100 MeV. The EOS outlined here has been applied recently to constrain the neutron-star radius [52] with a suggested range compatible with the best estimates from observations.

We show the EOSs used in this work in Fig. 1. The upper panel displays the total energy density, ϵ , as a function of baryon number density and the lower frame shows total pressure. Predictions from Akmal et al. [60] with the $A18 + \delta v + UIX^*$ interaction (APR) and recent DBHF calculations (Bonn B) [33, 34] with the Bonn B One-Boson-Exchange (OBE) potential are also shown. In addition to the pure nucleonic EOSs, we also include one hyperonic (Hyp) and one hybrid (Hyb) EOSs by the Catania group [80], see e.g. Ref. [82]. The hyperonic EOS shown in Fig. 1 is an updated version of the one reported in Ref. [81]. It has been calculated within the Brueckner-Hartree-Fock (BHF) approach using the Argonne v_{18} nucleon-nucleon (NN) potential, modified by nucleon three-body-forces according to the Urbana model, and

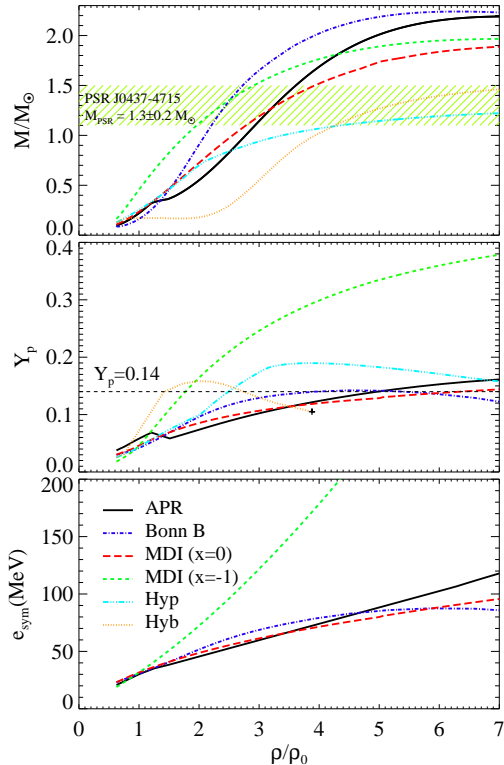


FIG. 2: (Color online) Neutron star mass, proton fraction, Y_p , and symmetry energy, e_{sym} . The upper frame displays the neutron star mass as a function of baryon number density. The middle frame shows the proton fraction and the lower frame the nuclear symmetry energy as a function of density. (Symmetry energy is shown for the nucleonic EOSs only.) The proton fraction curve of the Hyb EOS is terminated at the beginning of the quark phase. The termination point is denoted by a “cross” character.

with nucleon-hyperon interaction included. The hybrid EOS contains a BHF hadronic phase $(n, p, e, \mu, \Lambda, \Sigma)$ followed by a mixed phase $(n, p, e, \mu, \Lambda, \Sigma, u, d, s)$, and a pure quark phase (u, d, s, e) , calculated within the MIT bag model (with bag constant $B = 90 \text{ MeV fm}^{-3}$ and 150 MeV mass of the s-quark) [80]. The hadron-quark phase transition has been obtained by performing a Gibbs construction [80]. Since, as demonstrated in Refs. [46, 52], only equations of state with x between -1 and 0 have symmetry energies consistent with the isospin diffusion data and measurements of the skin thickness of ^{208}Rb , we thus consider only these two limiting cases. Below the density of approximately 0.07 fm^{-3} the equations of state shown in Fig. 1 are supplemented with a crust EOS [61, 62] which is more suitable for the low density regime.

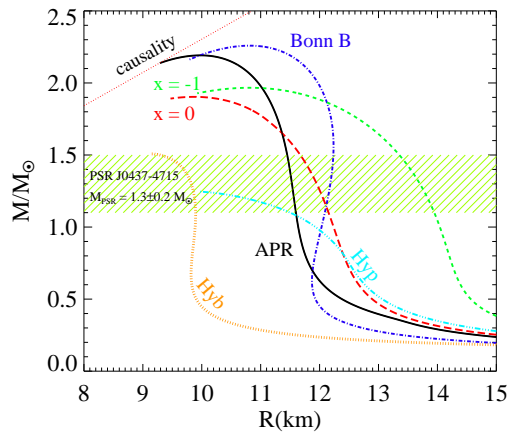


FIG. 3: (Color online) Mass-radius relation. The shaded region corresponds to the mass constraint from Hotan et al. [79].

TABLE 2: Maximum-mass neutron star models. The first column identifies the EOS. Remaining columns exhibit the following quantities for static configurations with maximum mass: total gravitational mass; radius; central baryon density.

EOS	$M_{max}(M_{\odot})$	$R(km)$	$\rho_c(fm^{-3})$
MDI($x=0$)	1.91	9.89	1.30
MDI($x=-1$)	1.97	10.85	1.08
Bonn B	2.24	10.88	1.08
APR	2.19	9.98	1.14
Hyp	1.25	9.96	1.49
Hyb (mixed phase)	1.51	9.14	1.50

Fig. 2 displays the neutron star mass (upper panel), the proton fraction (middle panel) and the nuclear symmetry energy (lower panel). The shaded region in the upper frame corresponds to the mass constraint by Hotan et al. [79]. From the neutron star models *satisfying this constraint* we observe that the proton fraction exceeds the direct URCA threshold for predictions from the $x = -1$ and Hyp EOSs. Here we recall that the fast URCA process proceeds only for Y_p above 0.14 due to simultaneous conservation of energy and momentum [63], causing rapid cooling of neutron stars. Hybrid stars (from the Hyb

EOS) cool rapidly through a quark direct URCA process (see Section V).

The corresponding stellar sequences are shown in Fig. 3. Table 2 summarizes the gravitational masses, radii and central densities of the *maximum-mass* configurations.

IV. CONSTRAINING THE CHANGING RATE OF THE GRAVITATIONAL CONSTANT G

To constrain the hypothetical time variation of G , we consider stellar models constructed from different equations of state and calculate the neutron star surface temperature via the gravitochemical heating method. Since only EOSs with x between -1 and 0 have symmetry energies consistent with terrestrial nuclear laboratory data [46, 52], we consider these two limiting cases as representative of the possible range of neutron star structures. As demonstrated by Jofré et al. [1], if one assumes only slow Urca reactions in the neutron star interior, the stellar photon luminosity and surface temperature in the stationary state can be evaluated through Eqs. (13) and (15) respectively. In the most general case, however, when both direct and modified Urca reactions operate in the neutron star interior (as for the $x = -1$, *Hyp* and *Hyb* EOSs), the analytic expression (13) becomes a very poor approximation [64]. Therefore, under this circumstance we calculate the surface temperature (and photon luminosity) in the quasi-equilibrium state by setting Eqs. (5), (8), and (9) to zero and solving them simultaneously.

In Fig. 4 we show the neutron star stationary photon luminosity (upper panel) and steady surface temperature (lower panel) versus stellar mass, assuming $|\dot{G}/G| = 4.5 \times 10^{-12} yr^{-1}$. The value of \dot{G} is chosen so that predictions from the $x = 0$ EOS are just above the 90% confidence contour of Kargaltsev et al. [22], see Fig. 5. This upper limit is consistent with the one by Jofré et al. [1] under the same assumptions. Here we reiterate that we apply the mass constraint by Hotan et al. [79] instead the one by van Straten et al. [23] used in Ref. [1]. (Both mass measurements partially overlap in the range $(1.4 - 1.5)M_{\odot}$.) We notice that predictions from the $x = 0$, APR and Bonn B EOSs all lie just above the observational constraints, with those from the $x = 0$ and APR EOSs being very similar to each other. This observation has been already made in a previous work [52] in conjunction with a study of the neutron star radius and was interpreted in terms of the good agreement between the

corresponding symmetry energies up to about $5\rho_0$ (see also Fig. 2, lower frame).

Figs. (6) and (7) display predictions assuming $|\dot{G}/G| = 2.1 \times 10^{-11} yr^{-1}$. In this case the value of \dot{G} is chosen so that predictions from the $x = -1$ EOS are just above the observational constraints. The surface temperature calculated with the $x = -1$ EOS is noticeably lower than predictions from EOSs allowing only modified Urca processes. This is due to opening of the fast Urca channel (see, Fig. 2, lower panel). When the neutron star mass becomes large enough for the central density to exceed the direct Urca threshold, the surface temperature drops because of the faster relaxation toward chemical equilibrium [1]. The upper limit we provide here is more restrictive than the one reported by Jofré et al. [1] in the case of fast cooling.

Before we close the discussion in this section we also compare our results with recent predictions from big bang nucleosynthesis (BBN) [70]. The stationary surface temperature in

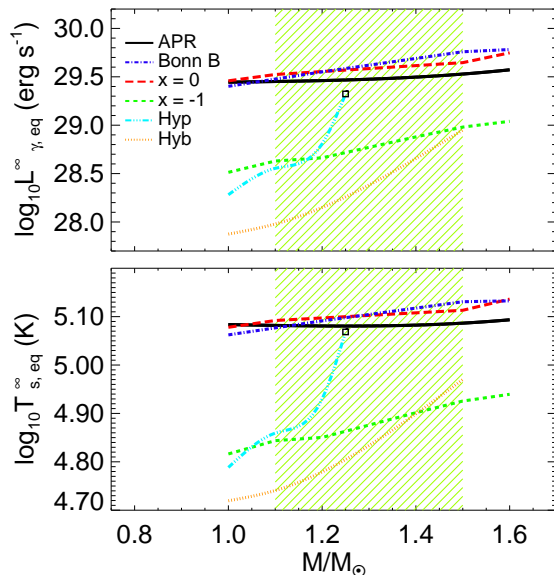


FIG. 4: (Color online) Stationary photon luminosity (upper frame) and neutron star surface temperature (lower frame) as functions of stellar mass, assuming $|\dot{G}/G| = 4.5 \times 10^{-12} yr^{-1}$. The shaded region corresponds to the mass constraint from Hotan et al. [79]. The open (black) square character denotes the maximum possible mass attained by the neutron star models constructed from the hyperonic EOS (Hyp). (The $x = -1$, *Hyp* and *Hyb* EOSs allow for fast cooling in the considered mass range. For the *Hyb* EOS, stellar cooling proceeds via a quark direct URCA process, see Section V.)

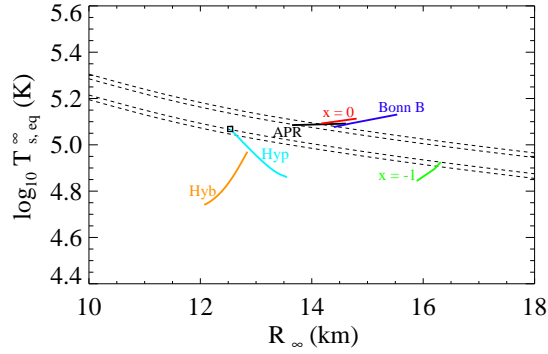


FIG. 5: (Color online) Neutron star stationary surface temperature for stellar models satisfying the mass constraint by Hotan et al. [79]. The solid lines are the predictions versus the stellar radius for the considered neutron star sequences. Dashed lines correspond to the 68% and 90% confidence contours of the black-body fit of Kargaltsev et al. [22]. The value of $|\dot{G}/G| = 4.5 \times 10^{-12} \text{yr}^{-1}$ is chosen so that predictions from the $x = 0$ EOS are just above the observational constraints.

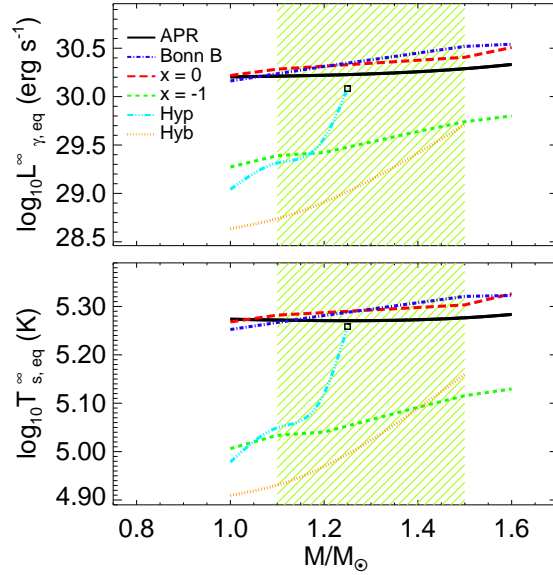


FIG. 6: (Color online) Same as Fig. 4 but now the value of $|\dot{G}/G| = 2.1 \times 10^{-11} \text{yr}^{-1}$ is chosen so that predictions from the $x=-1$ EOS are just above the observational constraints. (The $x = -1$ EOS allows direct Urca reactions in the considered mass range.)

Fig. 8 is calculated assuming $|\dot{G}/G| = 4 \times 10^{-13} \text{yr}^{-1}$ after Copi et al. [70]. We observe that in this case the resulting surface temperatures are below the observational contour of Kargaltsev

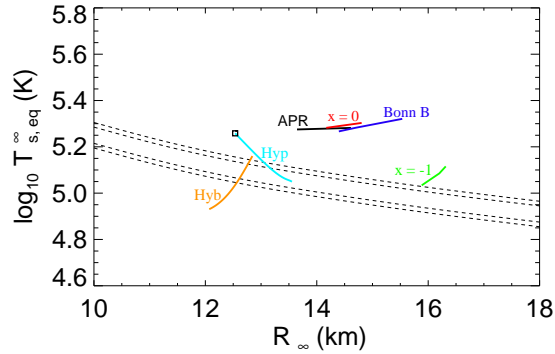


FIG. 7: (Color online) Same as Fig. 5 but assuming $|\dot{G}/G| = 2.1 \times 10^{-11} yr^{-1}$.

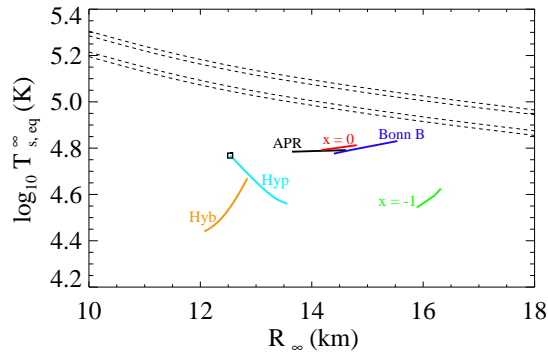


FIG. 8: (Color online) Same as Fig. 5 but assuming $|\dot{G}/G| = 4 \times 10^{-13} yr^{-1}$ after Copi et al. [70].

et al. [22]. There are several possible reasons which could account for this discrepancy: (i) The time scales of both methods are quite different. While the approach applied by Copi et al. [70] probes the constancy of G over the age of Universe (see Table 1), the gravitochemical heating method is sensitive to variations in G over shorter periods [1, 69], and falls closest to the second group of methods listed in Table 1. (ii) We do not consider the rotochemical heating [24] in this paper. On the other hand, the rotochemical heating, which is believed to play an important role in the thermal evolution of millisecond pulsars, cannot explain alone the observations of Kargaltsev et al. [22]. Therefore, additional heating mechanisms need to be considered [24]. In fact, if taken together the roto- and gravitochemical heatings could, in principle, explain the empirical surface temperature of PSR J0437-4715, where a smaller upper limit for $|\dot{G}/G|$ should be assumed [69]. Under this circumstance, our predictions

and those of Copi et al. [70] would be relatively close. (iii) Superfluidity is not taken into account. As pointed out in Refs. [1, 24, 69], this would raise the surface temperature due to lengthening the time-scales needed to reach equilibrium.

V. EFFECTS OF HYPERONS AND QUARKS

Although the major goal of our work is to constrain the changing rate of G by applying an EOS with constrained symmetry energy, our analysis would be incomplete without a discussion of the possible effects of “exotic” states of matter in neutron stars. Namely, in what follows we discuss the effects of hyperons and quarks.

Hyperons.- While at normal nuclear matter densities, $\rho \approx \rho_0$, neutron star matter consists of only nucleons and light leptons (e^- , μ^-), at higher densities several other species of particles are expected to appear due to the rapid rise of the baryon chemical potentials with density [81]. The first particles to appear after the muons are the Σ^- and Λ^0 hyperons. Strange baryons appear mainly in reactions such as [51]



The equilibrium conditions for these reactions read

$$2\mu_n = \mu_{\Sigma^-} + \mu_p \quad (22)$$

$$\mu_n = \mu_{\Lambda^0} \quad (23)$$

On the other hand, once the hyperons are present the following two chemical imbalances need to be introduced in addition to η_{npe} and $\eta_{np\mu}$ [24]

$$\eta_{2n\Sigma p} = 2\mu_n - \mu_{\Sigma^-} - \mu_p, \quad (24)$$

$$\eta_{n\Lambda} = \mu_n - \mu_{\Lambda^0} \quad (25)$$

Since processes (19) and (20) do not conserve strangeness, they can proceed only via weak interactions, while reactions (21) proceed via strong interactions. The above reactions have timescales at least several orders of magnitude shorter than those of beta processes [84] and,

therefore, $\eta_{2n\Sigma p}$ and $\eta_{n\Lambda}$ remain relatively small compared to η_{npe} and $\eta_{np\mu}$ [24]. Consequently, reactions (19)-(21) contribute negligibly to the total heat generation [24].

The importance of including Urca processes involving hyperons in the gravitochemical heating formalism, in addition to the nucleonic processes, can be assessed, for instance, by considering the following direct Σ^- Urca reactions [24]

$$\Sigma^- \rightarrow n + l + \bar{\nu}, \quad (26)$$

$$n + l \rightarrow \Sigma^- + \nu \quad (27)$$

The net effect of these processes on Eqs. (8) and (9) is to enhance the lepton direct Urca rates, reducing the chemical imbalances ($\eta_{npe}, \eta_{np\mu}$) and, in turn, the surface temperature. The overall correction is however small, because the direct Urca reactions with hyperons are at least a factor 5 weaker than the nucleon ones (see e.g. Prakash et al. [83]). For the case when only the modified Urca channel operates, Fernández et al. [24] showed that the correction to the surface temperature due to including several reactions involving hyperons is on the order of $[\tilde{L}_N/(\tilde{L}_N + \tilde{L}_H)]^{1/28}$, where \tilde{L}_N and \tilde{L}_H are the nucleon and hyperon Urca luminosities respectively. (This conclusion follows directly from Eq. (13).) Consequently, corrections due to hyperons in either direct or modified Urca processes can be neglected [24].

Yet, the inclusion of hyperons has a non-negligible effect on the EOS of neutron-star matter: Due to the appearance of additional degrees of freedom, the energy per particle is greatly reduced and the resulting EOS is much softer than its purely nucleonic counterpart [81, 82] (see also Fig. 1). This effect is entirely due to the inclusion of hyperons as additional degrees of freedom and is observed in all current calculations independent of the adopted many-body approach and/or interaction (see e.g. [82]). The consequences for the neutron star global properties, namely radii and masses, are reflected in an overall very large mass reduction with respect to models of $npe\mu$ -stars (Fig. 3).

Thus, in light of the above considerations, to investigate the impact of hyperons on the changing rate of G we apply a hyperonic EOS (see Section III) and the gravitochemical heating formalism without including the imbalances (24) and (25) (i.e., we do not consider openings of the hyperonic channels for additional heat emission). Rather, we aim to identify the effect of the global neutron star properties (masses and radii) from hyperonic EOS on the time variations of G in a qualitative way. In calculating the surface temperature we adopt a

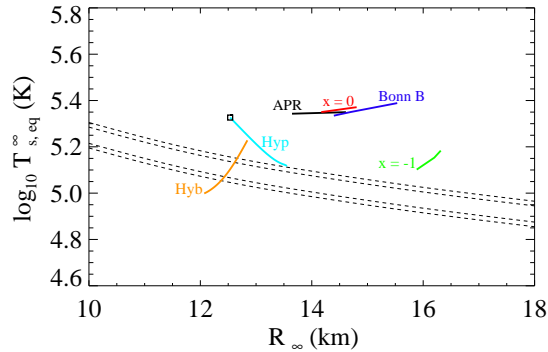


FIG. 9: (Color online) Same as Fig. 5 but assuming $|\dot{G}/G| = 3.6 \times 10^{-11} yr^{-1}$. The value of \dot{G} is chosen so that predictions from the hyperonic EOS (Hyp) are just above the empirical constraints.

fast cooling scenario since including of hyperonic degrees of freedom increases proton fraction above the threshold for fast *nucleonic* Urca processes for neutron stars in the considered mass range (see Fig. 2 upper and middle frames). We show our predictions for $|\dot{G}/G|$ based on the hyperonic EOS (Hyp) in Fig. 9. The value $|\dot{G}/G| = 3.6 \times 10^{-11} yr^{-1}$ reassures that results from the Hyp EOS are (just) above the empirical contours and is comparable with the one predicted with the $x = -1$ EOS (which also allows for fast Urca reactions). Here a few comments are in place: First, we should mention that due to the “softness” of the Hyp EOS, the maximum mass attained by the neutron star models in this case is much smaller than the corresponding masses predicted by purely nucleonic EOSs (see Fig. 3 and Table 1). The maximum mass is about $1.25M_{\odot}$ and falls closer to the lower limit of the allowed mass range for PSR J0437-4715. In fact, if one adopts the constraint by van Straten et al. [23] ($M_{PSR} = 1.58 \pm 0.18M_{\odot}$), M_{max} would be well below the allowed range. Also, as pointed out by Burgio et al. [82], a maximum mass less than $1.3M_{\odot}$ is in contradiction with the most precisely measured value of the Hulse-Taylor pulsar mass, PSR 1913+16, which amounts to $1.44M_{\odot}$; Second, hyperonic stars are much more compact than *npeμ*-stars. With the Hyp EOS the maximum mass is achieved at $\rho_c \approx 1.48 fm^{-3}$ (see Table 2). The rapid rise of the central density with increasing/decreasing neutron star mass/radius causes a steep growth in the predicted surface temperature (see e.g., Fig. 9); Finally, in the context of the gravitochemical heating of interest here, the only appreciable effect of hyperons is that their presence could facilitate the fulfilment of the direct Urca conditions, as in the

case of reactions involving Λ^0 [83]. Additionally, the rise of the proton fraction due to the appearance of Σ^- hyperons can shift the threshold of the nucleon direct Urca process to lower densities [85]. These considerations, together with the Hyp EOS predictions in Fig. 9, support the findings of Reisenegger [86], namely that the EOSs do not give very different results for the surface temperature if one only compares among those which either do or do not allow for direct Urca reactions.

Quarks.- The existence of quark matter in the interior of neutron stars is one of the major issues in the physics of these compact astrophysical objects. Here we discuss how the appearance of deconfined quarks would affect a possible time variation of G . For our analysis we choose a hybrid EOS (Hyb) derived by the Catania group (for details, see Section III and the references therein).

Quark matter is assumed to consist of deconfined u , d , and s quarks, and a small fraction of electrons [87]. At energies relevant to neutron stars, the u and d quarks are treated as massless particles, while the s quark is moderately relativistic and has a non-negligible mass [51]. The most important processes among the constituents of the quark-matter system are the direct Urca reactions with u and d quarks [51]

$$d \rightarrow u + e + \bar{\nu}_e, \quad (28)$$

$$u + e \rightarrow d + \nu_e \quad (29)$$

In addition, the following direct Urca reactions involving the s quark are possible:

$$s \rightarrow u + e + \bar{\nu}_e, \quad (30)$$

$$u + e \rightarrow s + \nu_e \quad (31)$$

These β -processes, however, do not conserve strangeness and, generally, yield much smaller emissivity relative to reactions (28) and (29) [51]. The chemical equilibrium conditions imply

$$\mu_d = \mu_s = \mu_u + \mu_e \quad (32)$$

A rigorous treatment of quark matter in the gravitochemical formalism would require major adjustments/extensions of the framework to incorporate, for instance, the imbalances η_{ued} and η_{ues} , and the corresponding quark emissivities. Since this task is beyond the main focus of this work, we take a much simpler approach which should, at minimum, hint on

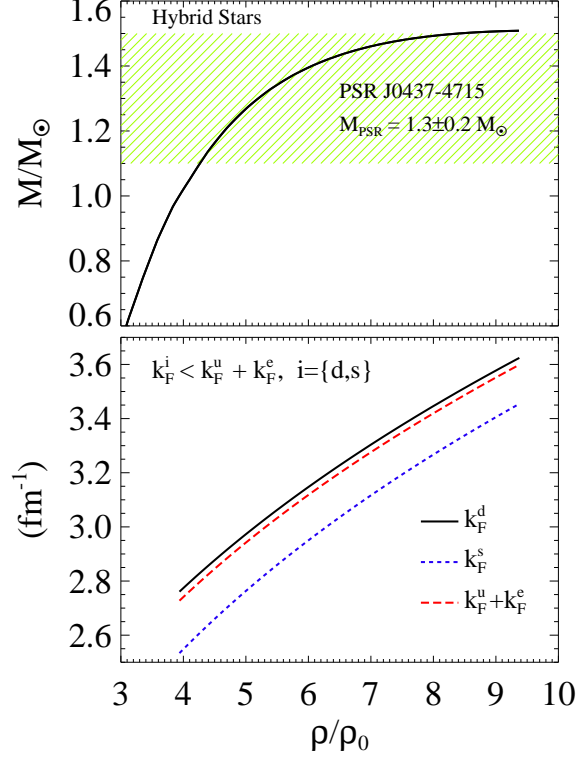


FIG. 10: (Color online) Models of hybrid stars (upper frame) and triangle inequality (lower frame).

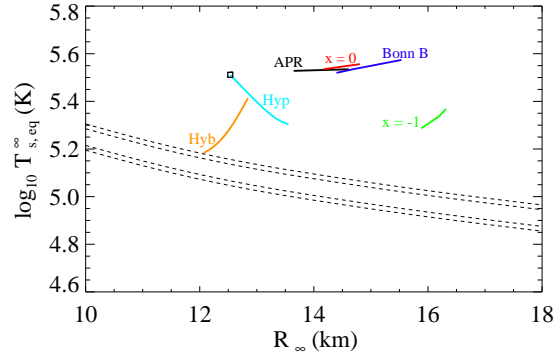


FIG. 11: (Color online) Same as Fig. 5 but assuming $|\dot{G}/G| = 1.6 \times 10^{-10} \text{yr}^{-1}$. The value of \dot{G} is chosen so that predictions from the hybrid EOS (Hyb) are just above the empirical constraints.

the effect of quarks relative to the $npe\mu$ -matter. Similarly to what is done in the case of hyperonic stars, we provide a (qualitative) estimate based on the mass-radius correlation of hybrid stars, rather than their detailed composition. Because the triangle inequality

$$k_F^i < k_F^u + k_F^e, \quad i = \{d, s\} \quad (33)$$

among the Fermi momenta of species u , d , s and e , is fulfilled for reactions (30) and (31) but is not for (28) and (29) (see Fig. 10), cooling of hybrid stars (from the Hyb EOS) can proceed through quark direct Urca processes involving the s quark. Therefore we assume a fast-cooling scenario. Our predictions for $|\dot{G}/G|$ based on the Hyb EOS are shown in Fig. 11. We notice that the value $|\dot{G}/G| = 1.6 \times 10^{-10} yr^{-1}$ (chosen so that predictions from the Hyb EOS are above the empirical data) falls closest to the one derived by Jofre et al. [1] under the modified Urca assumption (and also our predictions from the $x = -1$ and *Hyp* EOSs). Since the yield of reactions (30) and (31) is less certain [51] and because we do not treat the inclusion of quarks explicitly, we should keep in mind that the present result is more qualitative than quantitative and therefore more refined calculations might be necessary to draw more definite conclusions. On the other hand, we observe a steep rise of surface temperature with stellar mass (red-shifted radius and/or central density), see e.g. Fig. 11. The rapid temperature increase is attributed to the fast growth of central density with mass (Fig. 10, upper panel), and has been already observed in conjunction with the analysis of hyperonic stars (see above). Finally, we notice that hybrid stars have, generally, smaller radii than those of $npe\mu$ -stars (Fig. 3). In fact, the radii predicted with the Hyb EOS employed here are below the latest neutron star radius constraints [52] (see also Fig. 3). Yet, models yielding quite stiff quark matter EOSs, and, in turn, hybrid/quark star radii (masses) consistent with the latest observations [66], do exist [88]. Given the large present uncertainties in modeling the quark phase of matter, our results provide a reasonable qualitative assessment of the changing rate of G , based on the gravitochemical heating method and a hybrid EOS.

VI. SUMMARY

In summary, to test the Dirac hypothesis and constrain the changing rate of the gravitational constant G due to the continuous expansion of the Universe, we have calculated the neutron star surface temperature through the gravitochemical formalism introduced by Jofré et al. [1] applying several EOSs spanning from pure nucleonic matter to quark matter. One of the nucleonic EOSs has a density dependence of the symmetry energy constrained by terrestrial nuclear laboratory data that just became available recently. Using the “softer”

symmetry energy ($x = 0$) consistent with both the isospin diffusion and the ^{208}Pb neutron skin data, we obtain an upper limit $|\dot{G}/G| \leq 4.5 \times 10^{-12} \text{yr}^{-1}$ compatible with that obtained by Jofré et al. [1] under the same assumptions. This is mainly because the density dependence of the symmetry energy with $x = 0$ turns out to be very close to that with the APR EOS they also used. The “stiffer” symmetry energy ($x = -1$) EOS yields an upper limit $|\dot{G}/G| \leq 2.1 \times 10^{-11} \text{yr}^{-1}$, an order of magnitude lower than the one derived by Jofré et al. [1] when both direct and modified Urca reactions operate. Since both the $x = 0$ and $x = -1$ equations of state have symmetry energies consistent with the empirical nuclear data, we cannot rule out the results from the direct Urca scenario. In the case of fast cooling, our result provides even tighter upper limit than the one reported in Ref. [1].

The gravitochemical heating mechanism has the potential to become a powerful tool for constraining gravitational physics. Since the method relies on the detailed neutron star structure, which, in turn, is determined by the EOS of stellar matter, further progress in our understanding of properties of dense, neutron-rich matter will make this approach more effective. Precise astrophysical observations such as those by Özel [66], Hessels et al. [65], and Kaaret et al. [67] together with future heavy-ion experiments with high energy radioactive beams [68] will allow us to set more stringent constraints on the EOS of dense neutron-rich matter, and on the possible time variation of the gravitational constant G .

Acknowledgements

We would like to thank Rodrigo Fernández and Andreas Reisenegger for helpful discussions and assistance with the numerics. We also thank Fiorella Burgio for providing the hyperonic and hybrid EOSs. This work was supported by the National Science Foundation under Grant No. PHY0652548 and the Research Corporation under Award No. 7123.

-
- [1] P. Jofre, A. Reisenegger and R. Fernandez, Phys. Rev. Lett. **97**, 131102 (2006).
 - [2] P. A. M. Dirac, Nature **139**, 323 (1937).
 - [3] C. Brans and R. H. Dicke, Phys. Rev. **124**, 925 (1961).

- [4] E. Garcia-Berro, Yu. A. Kubyshin, P. Loren-Aguilar and J. Isern, *Int. J. Mod. Phys. D* **15**, 1163 (2006) [arXiv:gr-qc/0512164].
- [5] L. M. Krauss and M. S. Turner, *Gen. Rel. Grav.* **27**, 1137 (1995).
- [6] A. Bonanno and M. Reuter, *Phys. Lett. B* **527**, 9 (2002).
- [7] J. M. Overduin and P. S. Wesson, *Phys. Rept.* **283**, 303 (1997).
- [8] P. Horava and E. Witten, *Nucl. Phys. B* **460**, 506 (1996).
- [9] T. Damour, F. Piazza and G. Veneziano, *Phys. Rev. Lett.* **89**, 081601 (2002).
- [10] T. Damour, F. Piazza and G. Veneziano, *Phys. Rev. D* **66**, 046007 (2002).
- [11] I. Zlatev, L. M. Wang and P. J. Steinhardt, *Phys. Rev. Lett.* **82**, 896 (1999).
- [12] C. Armendariz-Picon, V. F. Mukhanov and P. J. Steinhardt, *Phys. Rev. Lett.* **85**, 4438 (2000).
- [13] C. Armendariz-Picon, V. F. Mukhanov and P. J. Steinhardt, *Phys. Rev. D* **63**, 103510 (2001).
- [14] P. J. Steinhardt, L. M. Wang and I. Zlatev, *Phys. Rev. D* **59**, 123504 (1999).
- [15] A. Hebecker and C. Wetterich, *Phys. Rev. Lett.* **85**, 3339 (2000).
- [16] A. Hebecker and C. Wetterich, *Phys. Lett. B* **497**, 281 (2001).
- [17] S. Chandrasekhar, *Nature* **139**, 757 (1937).
- [18] D.S. Kothari, *Nature* **142**, 354(1938).
- [19] S. Perlmutter *et al.* [Supernova Cosmology Project Collaboration], *Astrophys. J.* **517**, 565 (1999).
- [20] A. G. Riess, *Publ. Astron. Soc. Pac.* **112**, 1284 (2000).
- [21] J. P. Uzan, *Rev. Mod. Phys.* **75**, 403 (2003).
- [22] O. Kargaltsev, G. G. Pavlov and R. W. Romani, *Astrophys. J.* **602**, 327 (2004).
- [23] W. van Straten, M. Bailes, M. C. Britton, S. R. Kulkarni, S. B. Anderson, R. N. Manchester and J. Sarkissian, *Nature* **412**, 158 (2001) [arXiv:astro-ph/0108254].
- [24] R. Fernandez and A. Reisenegger, *Astrophys. J.* **625**, 291 (2005).
- [25] A. Reisenegger, *Astrophys. J.* **442**, 749 (1995).
- [26] J. M. Lattimer and M. Prakash, *Phys. Rept.* **333**, 121 (2000).
- [27] J. M. Lattimer and M. Prakash, *Science* **304**, 536 (2004).
- [28] M. Prakash, J. M. Lattimer, R. F. Sawyer and R. R. Volkas, *Ann. Rev. Nucl. Part. Sci.* **51**, 295 (2001).
- [29] D. G. Yakovlev and C. J. Pethick, *Ann. Rev. Astron. Astrophys.* **42**, 169 (2004).

- [30] H. Heiselberg and V. Pandharipande, *Ann. Rev. Nucl. Part. Sci.* **50**, 481 (2000).
- [31] H. Heiselberg and M. Hjorth-Jensen, *Phys. Rept.* **328**, 237 (2000).
- [32] A. W. Steiner, M. Prakash, J. M. Lattimer and P. J. Ellis, *Phys. Rept.* **411**, 325 (2005).
- [33] D. Alonso and F. Sammarruca, *Phys. Rev. C* **67**, 054301 (2003).
- [34] P. Krastev and F. Sammarruca, *Phys. Rev. C* **74**, 025808 (2006).
- [35] B. A. Li, C. M. Ko and Z. Ren, *Phys. Rev. Lett.* **78**, 1644 (1997).
- [36] B. A. Li, *Phys. Rev. Lett.* **85**, 4221 (2000).
- [37] B. A. Li, *Phys. Rev. Lett.* **88**, 192701 (2002).
- [38] B. A. Li, C. M. Ko and W. Bauer, *Int. J. Mod. Phys. E* **7**, 147 (1998).
- [39] B. A. Li and W. Udo Schroeder (Eds.) *Isospin Physics in Heavy-Ion Collisions at Intermediate Energies*, Nova Science, New York (2001).
- [40] P. Danielewicz, R. Lacey and W. G. Lynch, *Science* **298**, 1592 (2002).
- [41] V. Baran, M. Colonna, V. Greco and M. Di Toro, *Phys. Rept.* **410**, 335 (2005).
- [42] L. Shi and P. Danielewicz, *Phys. Rev. C* **68**, 064604 (2003).
- [43] M.B. Tsang et al., *Phys. Rev. Lett.* **92**, 062701 (2004).
- [44] L. W. Chen, C. M. Ko and B. A. Li, *Phys. Rev. Lett.* **94**, 032701 (2005).
- [45] A. W. Steiner and B. A. Li, *Phys. Rev. C* **72**, 041601 (2005).
- [46] B. A. Li and L. W. Chen, *Phys. Rev. C* **72**, 064611 (2005).
- [47] L. W. Chen, C. M. Ko and B. A. Li, *Phys. Rev. C* **72**, 064309 (2005).
- [48] C. J. Horowitz and J. Piekarewicz, *Phys. Rev. Lett.* **86**, 5647 (2001).
- [49] C. J. Horowitz and J. Piekarewicz, *Phys. Rev. C* **66**, 055803 (2002).
- [50] B. G. Tod-Rutel and J. Piekarewicz, *Phys. Rev. Lett.* **95**, 122501 (2005).
- [51] D. G. Yakovlev, A. D. Kaminker, O. Y. Gnedin, P. Haensel, *Phys. Rep.* **354**, 1-155 (2001).
- [52] B. A. Li and A. W. Steiner, *Phys. Lett. B* **642**, 436 (2006).
- [53] C. B. Das, S. D. Gupta, C. Gale and B. A. Li, *Phys. Rev. C* **67**, 034611 (2003).
- [54] U. Garg, nucl-ex/0608007.
- [55] R. B. Wiringa, *Phys. Rev. C* **38**, 2967 (1988).
- [56] F. Sammarruca, W. Barredo and P. Krastev, *Phys. Rev. C* **71**, 064306 (2005).
- [57] G. M. Welke, M. Prakash, T. T. S. Kuo, and S. Das Gupta, *Phys. Rev. C* **38**, 2101 (1988).
- [58] C. Gale, G.M. Welke and M. Prakash et al., *Phys. Rev. C* **41**, 1545 (1990).

- [59] J. Zhang, S. Das Gupta and C. Gale, Phys. Rev. C **50**, 1617 (1994).
- [60] A. Akmal, V. R. Pandharipande and D. G. Ravenhall, Phys. Rev. C **58**, 1804 (1998).
- [61] C. J. Pethick, D. G. Ravenhall and C. P. Lorenz, Nucl. Phys. A. **584**, 675-703 (1995).
- [62] P. Haensel and B. Pichon, Astron. Astrophys. **283**, 313-318 (1994).
- [63] J. M. Lattimer, M. Prakash, C. J. Pethick and P. Haensel, Phys. Rev. Lett. **66**, 2701 (1991).
- [64] R. Fernández, private communications.
- [65] J. W. T. Hessels, S. M. Ransom, I. H. Stairs, P. C. C. Freire, V. M. Kaspi and F. Camilo, Science **311**, 1901–1904 (2006).
- [66] F. Özel, Nature **441**, 1115-1117 (2006).
- [67] P. Kaaret, Z. Prieskorn, J. J. M. in 't Zand, S. Brandt, N. Lund, S. Mereghetti, D. Götz, E. Kuulkers, and J. A. Tomsick, Astrophys. J. **657**, L97-L100 (2007).
- [68] RIA Theory Bluebook, <http://www.orau.org/ria/RIATG>.
- [69] A. Reisenegger, R. Fernandez and P. Jofre, Astrophys. Space Sci., **308**, 413-418 (2007); astro-ph/0610955.
- [70] C. Copi, A. Davis and L. Krauss, Phys. Rev. Lett. **92**, 17 (2004).
- [71] R. Nagata, T. Chiba and N. Sugiyama, Phys. Rev. D **69**, 3512 (2004).
- [72] S. Degl'Innocenti et al., Astron. Astrophys. **312**, 345 (1996).
- [73] S. E. Thorsett, Phys. Rev. Lett. **77**, 1432 (1996).
- [74] D. B. Guenther, L. M. Krauss and P. Demarque, Astrophys. J. **498**, 871 (1998).
- [75] W. Eichendorf and M. Reinhardt, Mitteilungen der Astronomischen Gesellschaft Hamburg, **42**, 89 (1977) (result cited in Ref. [21]).
- [76] J. G. Williams, S. G. Turyshev and D. H. Boggs, Phys. Rev. Lett. **93**, 261101-1-4 (2004).
- [77] V. M. Kaspi, J. H. Taylor and M. .F. Ryba, Astrophys. J. **428**, 713 (1994).
- [78] O. Benvenuto, E. Garcia-Berro and J. Isern., Phys. Rev. D **69**, 2002 (2004).
- [79] A. W. Hotan, M. Bailes and S. M. Ord, Mon. Not. R. Astron. Soc. **369**, 15021520 (2006).
- [80] G. F. Burgio, private communications.
- [81] M. Baldo, G. F. Burgio and H. -J. Schulze, Phys. Rev. C **61**, 055801 (2000).
- [82] G. F. Burgio, nucl-th/0707.4067.
- [83] M. Prakash, M. Prakash, J. M. Lattimer, and C. J. Pethick, Astrophys. J. **390**, L77 (1992).
- [84] W. D. Langer and A. G. W. Cameron, Astrophys. Space Sci., **5**, 213 (1969).

- [85] N. K. Glendenning, *Compact Stars, Nuclear Physics, Particle Physics, and General Relativity*, Springer-Verlag New York, Inc. (1997).
- [86] A. Reisenegger, private communications.
- [87] C. Maieron, M. Baldo, G.F. Burgio, and H.-J. Schulze, Phys. Rev. D **70**, 043010 (2004).
- [88] M. Alford, M. Braby, M. Paris, and S. Reddy, Astrophys. J. **629**, 969-978 (2005).